Generalized fracture toughness for specimens with re-entrant corners: Experiments vs. theoretical predictions

Alberto Carpinteri, Pietro Cornetti, Nicola Pugno and Alberto Sapora†

Department of Structural Engineering and Geotechnics, Politecnico di Torino, Turin, Italy

David Taylor

Department of Mechanical and Manufacturing Engineering, Trinity College, Dublin 2, Ireland

(Received December 11, 2008, Accepted June 14, 2009)

Abstract. In this paper the results of a series of experimental tests upon three-point bending specimens made of polystyrene and containing re-entrant corners are firstly described. Tests involved different notch angles, different notch depths and finally different sizes of the samples. All the specimens broke at the defect, as expected because of the material brittleness and, hence, the generalized stress intensity factor was expected to be the governing failure parameter. Recorded failure loads are then compared with the predictions provided by a fracture criterion recently introduced in the framework of Finite Fracture Mechanics: fracture is assumed to propagate by finite steps, whose length is determined by the contemporaneous fulfilment of energy balance and stress requirements. This fracture criterion allows us to achieve the expression of the generalized fracture toughness as a function of the tensile strength, the fracture toughness and the notch opening angle. Comparison between theoretical predictions and experimental data turns out to be more than satisfactory.

Keywords: three-point bending test; V-notch; fracture toughness; tensile strength; Finite Fracture Mechanics.

1. Introduction

Criteria assuming that failure of quasi-brittle materials is affected by the stresses acting at a finite distance from the crack tip are widely used inside the Scientific Community. These approaches can be grouped together under the general term of Theory of Critical Distances (Taylor 2004), in which linear-elastic analysis is combined with a material-dependent length. Among these criteria, the most common is the average stress criterion, which assumes as a critical parameter the average stress over a characteristic material length ahead of the crack tip. It dates back to Neuber (1958) and Novozhilov (1969), and, afterwards, several researchers have applied it in a wide range of geometries and materials: see, for instance, notch analysis (Seweryn 1995, Carpinteri and Pugno

† Corresponding author, E-mail: alberto.sapora@polito.it

2005) and fatigue problems (Taylor 1999). However, this kind of criteria disregards energy balance considerations which, as well known, are the basis of the Linear Elastic Fracture Mechanics.

On the other hand, the novelty of the criterion used in the present paper and proposed by Cornetti *et al.* (2007) relies on the simultaneous fulfilment of energy balance and stress requirement under the assumption of a finite crack extension: i.e., failure is achieved whenever there is a segment of length Δ ahead of the notch tip over which the stress resultant is equal to $\sigma_u \Delta$, and, contemporarily, the energy available for that crack extension is equal to $G_F \Delta$; σ_u and G_F are the material tensile strength and fracture energy, respectively. Differently from the average stress criterion, the length Δ is no more a material constant but a structural parameter, thus able to take the interaction between the finite crack extension and the geometry of the specimen into account. Henceforth, we refer to this criterion as the coupled Finite Fracture Mechanics (FFM) criterion. Aim of the present paper is to present experimental results obtained testing V-notched specimens and to show that satisfactory theoretical predictions may be obtained by exploiting the coupled FFM criterion.

The plan of the paper is as follows. In Section 2, the results of a series of experimental tests upon three-point bending specimens made of polystyrene and containing re-entrant corners are firstly described. Tests involved different notch angles, different notch depths and finally different sizes of the samples. In Section 3, the basic equations of the coupled FFM criterion are briefly outlined and its particularization to determine the strength of a V-notched specimen is recalled (Carpinteri *et al.* 2008). Eventually, in Section 4 it is shown that theoretical predictions are in a fair agreement with the experimental data obtained.

2. Three-point bending tests of V-notched specimens

A series of tests with notched three-point bending specimens made of polystyrene was carried out. Note that data about polystyrene specimens are not so common in the literature. Although brittle for usual laboratory sizes, polystyrene is less brittle than PMMA, which is considered as the archetype of brittle polymers, and for which a large amount of data is already available (see e.g., Carpinteri 1987, Seweryn 1994, Dunn *et al.* 1997).

2.1 Description of the tests

The specimen geometry is as in Fig. 1. Three kinds of tests were performed by varying the notch angle ω (*test 1*), the notch depth d (*test* 2) and the specimen dimensions l, b and d in a proportional

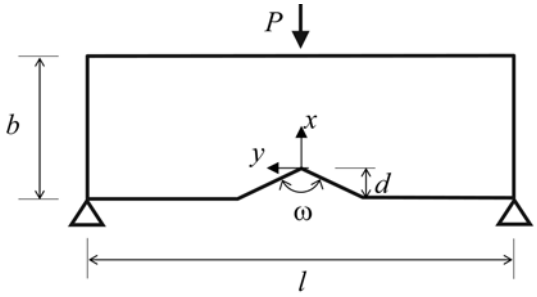

Fig. 1 Three-point bending test of a V-notched specimen

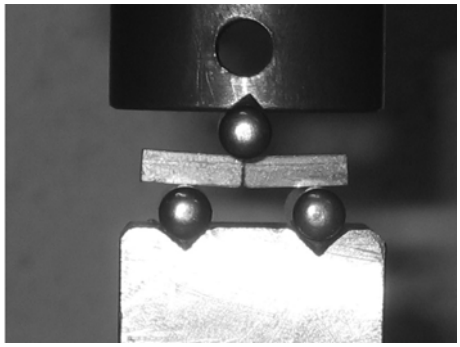

Fig. 2 Three-point bending test of a polystyrene beam (test 3)

way (*test 3*), respectively.

Notched flexure specimens were initially obtained from a polystyrene sheet with the following dimensions: the thickness t was equal to 3.7 mm (which is enough to get plane strain conditions); the length l and the height b were equal to 76 and 18 mm.

The notch wedge angles were $\omega = 60^o$, 120^o and 150^o. A notch depth of $d = 1.8$ mm ($d/b = 1/10$) was firstly machined for each of the three notch angles mentioned (*test 1*). Then, for the 120^o-notch samples, three other notch depths were machined: $d = 0.2$, 0.6 and 10.8 mm. These values yield d/b ratios of 1/90, 1/30 and 6/10, respectively (*test 2*). Finally, keeping the notch angle ω fixed to 120^o and the relative notch depth d/b to 1/10, all the specimen dimensions (except the thickness t) were decreased by a factor of five. This corresponds to: $l = 15.2$ mm, $b = 3.6$ mm, $d = 0.36$ mm (*test 3*, Fig. 2).

Five identical specimens were tested for each of the seven geometries contemplated. Moreover, five plain specimens were tested to obtain the tensile strength value σ_u, which was found equal to 70.6 MPa. i.e., a total of forty specimens was tested. Anyway, beyond the tensile strength, also the fracture toughness is required to predict the failure load according to the coupled FFM criterion (see Section 3). This was not obtained experimentally. Thus a best fit procedure exploiting the data of all the notched specimens was used to get its value (an analogous procedure was used by Seweryn (1995)): $K_{Ic} = 2.23$ MPa m.

Test 1 and *test 2* were carried out at a strain rate of 10 mm/min. On the other hand, a different machine was used to carry out *test 3* because of the lower distance between the two supports: specimens were tested under a strain rate of 1 mm/min.

Specimens were machined in order to have a V-notch as sharp as possible. They were then checked with a measuring microscope: the maximum notch root radius was equal to 0.02 mm for the geometry with $\omega = 60^o$; in all the other cases, it was smaller than 10 mm, i.e., the instrument precision. Therefore, in the theoretical analysis, we considered the notch as perfectly sharp, i.e., we assumed that the test results are not affected by so small notch root radii.

To what concerns *test 1*, note that the specimen dimensions are similar to those tested by Dunn *et al.* (1997). They carried out three-point bending tests on PMMA samples with notch opening angles equal to 60^o, 90^o and 120^o.

On the other hand, cases considered in *test 2* are interesting since they represent the limit cases for the criteria based on the generalized fracture toughness to work, i.e., very small and very large notch depths.

Eventually, *test 3* was carried out to catch the well known size scale effects (Carpinteri 1987), i.e., embrittlement of the structural response as the size increases.

2.2 Experimental results and physical considerations

Critical values of the load under which crack begins to propagate from the notch vertex, recorded on the bending testing machine, are given in Table 1, Table 2 and Table 3 for *test 1*, *test 2* and *test 3*, respectively. The divergence of the standard deviation over the average is relatively small in all the cases, the maximum deviation being 6.3%. This highlights the good repeatability in the tests and the small scatter experienced.

It is observed that the critical load increases as the notch angle increases and/or as the notch depth decreases. Anyway, there is not a significant difference between the failure load for the 60°-notch samples and the 120°-notch samples. This interesting result will be confirmed by theoretical analysis.

The polystyrene fracture was of brittle character and no plastic strains were observed in *test 1* and *2*: all the specimens broke at the defect. On the contrary, a more ductile behaviour was observed during *test 3*: the two pieces into which specimens used to shatter, always remained attached after failure, revealing the presence of a plastic hinge. Anyway this is not so surprising if we refer to the brittleness number s

Table 1 Results test 1: critical failure load [N] for polystyrene specimens with different notch opening angles ω (d/b = 0.1) and coefficient of variation (standard deviation/average)

ω	1	2	3	4	5	Avg.	St.Dev./Avg.
60°	332.0	322.9	319.5	345.0	293.2	322.5	0.06
120°	317.7	342.2	324.7	320.2	308.7	322.7	0.04
150°	369.2	327.0	327.0	345.5	340.5	341.8	0.05

Table 2 Results test 2: critical failure load [N] for polystyrene specimens with different notch depths d/b (ω = 120°) and coefficient of variation (standard deviation/average)

d/b	1	2	3	4	5	Avg.	St.Dev./Avg.
0	751.0	779.5	809.2	739.8	775.0	770.9	0.03
1/90	592.2	520.0	507.7	518.5	526.5	533.0	0.06
1/30	456.5	453.1	414.0	446.5	445.0	443.0	0.04
1/10	317.7	342.2	324.7	320.2	308.7	322.7	0.04
6/10	60.0	60.4	57.9	62.4	63.3	60.8	0.03

Table 3 Results test 3: critical failure load [N] for polystyrene specimens with different sizes (d/b = 0.1, ω = 120°) and coefficient of variation (standard deviation/average)

Scaling factor	1	2	3	4	5	Avg.	St.Dev./Avg.
1	317.7	342.2	324.7	320.2	308.7	322.7	0.04
0.2	107.8	109.1	106.0	113.2	102.0	107.6	0.03

$$s = \frac{K_{Ic}}{\sigma_u \sqrt{b}} \tag{1}$$

where b is a characteristic length of the structure, e.g., the specimen height in the present case. The brittleness number s is a non-dimensional quantity, introduced by Carpinteri (1981), which describes in a unitary and synthetic manner the embrittlement of the structural response as the size increases. Brittle structural behaviours are generally expected for low brittleness numbers (Carpinteri *et al.* 2003). In the next sections, predictions will refer to a brittleness number $s = 0.236$ for samples of *test 1* and *test 2* and $s = 0.503$ for samples of *test 3*.

3. Coupled finite fracture mechanics criterion

As stated in the introduction, the average stress criterion disregards energy balance. To overcome this shortcoming, a criterion according to which fracture propagates when the energy available for a finite crack advance reaches a critical value was recently proposed (Pugno and Ruoff 2004, Taylor *et al.* 2005). This approach was named Finite Fracture Mechanics and represents the energy counterpart of the average stress criterion. It should be noted that FFM bypasses the stress requirements for crack growth. However the two approaches, i.e., the energetic and the stress criterion, can be satisfied contemporaneously by removing the assumption that the finite crack extension is constant (Leguillon 2002, Cornetti *et al.* 2007). According to the coupled FFM criterion, failure takes place whenever (Cornetti *et al.* 2007)

$$\begin{cases} \int_0^{\Delta} \sigma_y(x)\mathrm{d}x = \sigma_u \Delta \\ \int_0^{\Delta} K_I^2(a)\mathrm{d}a = K_{Ic}^2 \Delta \end{cases} \tag{2}$$

where x is the direction of crack growth and $x = 0$ corresponds to the notch tip (see, e.g., Fig. 1), $\sigma_y(x)$ is the stress normal component directed along the y-axis, a the crack length, $K_I(a)$ the stress intensity factor (SIF) and Δ the finite crack extension. The first equation is the stress requirement for crack propagation and, provided that Δ is no more a material constant, it coincides with the average stress criterion. On the other hand, the second equation represents the energy balance, since, dividing both sides by the Young modulus in plane strain condition E', the integrand function at the left hand side is the strain energy release rate and, at the right hand side, the fracture energy appears according to Irwin's relationship ($G_F = K_{Ic}^2/E'$).

Eq. (2) represents a system of two equations in the two unknowns: σ_f i.e., the failure load (implicitly embedded in the functions $\sigma_y(x)$ and $K_I(a)$), and Δ, i.e., the crack extension. While each single equation represents only a necessary condition for failure, the fulfilment of both of them represents a necessary and sufficient condition for fracture to propagate. From a physical point of view, the criterion expressed in Eq. (2) is equivalent to state that fracture is energy driven but a sufficiently high stress field must act in order to trigger crack propagation.

In this Section the coupled FFM criterion is applied to the strength prediction of TPB specimens with a V-notch at a mid-span. Let us consider the specimen geometry of Fig. 1. By means of

Table 4 Values of the shape function f (Eq. (4)) for different notch opening angles ω (d/b = 0.1)

ω	0°	30°	60°	90°	120°	150°	180°
f	0.8250	0.8356	0.8761	0.9749	1.1618	1.4453	1.7819

Table 5 Values of the shape function f (Eq. (4)) for different notch depths d/b (ω = 120°)

d/b	1/90	1/30	1/10	3/10	6/10	9/10
f	0.5438	0.8046	1.1617	1.9129	4.8526	46.408

dimensional analysis it is possible to write the generalized SIF as:

$$K_I^* = \frac{Pl}{tb^{1+\lambda}} f\left(\frac{l}{b}, \frac{d}{b}, \omega\right) \tag{3}$$

where f is the so-called shape function and λ is an exponent which depends on the angle ω according to the classical Williams' analysis: $\lambda = \lambda(\omega)$. In order to compute the values of the shape function f, the value of the generalized SIF K_I^* for unit load is needed. Therefore a FEA was performed by using the LUSAS ® code for each tested geometry. Then, by means of the H-integrals (Sinclair *et al.* 1984), the relative SIFs were evaluated leading to the values of f (Tables 4 and 5) to be inserted into Eq. (3).

Because of structural brittleness, the governing failure parameter is expected to be K_I^*, i.e., the coefficient of the dominant term of the stress field at the notch tip. In other words, we assume that failure takes place whenever $K_I^* = K_{Ic}^*$, where K_{Ic}^* is the generalized toughness. Therefore, in critical conditions, Eq. (3) becomes

$$K_{Ic}^* = \frac{P_{cr}^{\omega} l}{tb^{1+\lambda}} f\left(\frac{d}{b}, \omega\right) \tag{4}$$

and, if ω = 180°, yields

$$\sigma_u = \frac{P_{cr}^{\pi} l}{tb^2} f\left(\frac{d}{b}, \pi\right) \tag{5}$$

where P_{cr}^{ω} and P_{cr}^{π} are the failure loads for a notch opening angle equal to ω and to 180°, respectively. For the sake of simplicity, the dependence of the shape function on the specimen slenderness l/b is not given explicitly, since it was kept constant in all the tests. Moreover, note that the value of f corresponding to ω = 180° can be found in structural mechanics classical books (it provides the maximum normal stress for an un-notched TPB specimen, whose height is b-d).

The coupled FFM criterion is now applied to determine the values of the generalized toughness as a function of the notch opening angle ω. To this purpose, it is necessary to find the expressions for the stress field $\sigma_y(x)$ and for the SIF $K_I(a)$ to be inserted into the system (2). If the crack advancement Δ is small enough with respect to the other geometrical quantities, the stress field $\sigma_y(x)$ can be sufficiently well described by its asymptotic expansion

$$\sigma_y(x) = \frac{K_I^*}{(2\pi x)^{1-\lambda}} \tag{6}$$

On the other hand, the SIF $K_I(a)$ can be obtained from the weight functions providing the SIF for

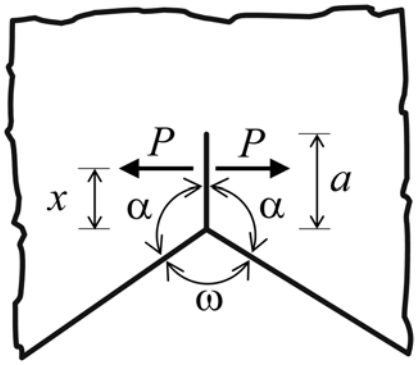

Fig. 3 Crack at a V-notch tip loaded by a pair of forces P

a crack at a V-notch tip of an infinite plate loaded by a pair of forces acting on the crack lips (see Fig. 3). Note that this geometry is not the actual one. Nevertheless, assuming a brittle structural behaviour (low brittleness number), the finite crack extension is much shorter than the other specimen geometrical quantities: the two geometries tend, hence, to coincide.

The SIF for a pair of forces P is (Tada *et al*. 1985)

$$K_I = P\sqrt{2/(\pi a)}\, F(x/a, \alpha) \tag{7}$$

with

$$F(x/a, \alpha) = \frac{\tilde{f}(\alpha) + (x/a)\tilde{g}(\alpha) + (x/a)^2\tilde{h}(\alpha)}{\sqrt{1 - x/a}} \tag{8}$$

where $\alpha = \pi - \omega/2$ (see Fig. 3). The expressions of the functions $\tilde{f}, \tilde{g}$ and $\tilde{h}$ are as follows

$$\tilde{f}(\alpha) = \sqrt{\frac{\pi}{2}}\sqrt{\frac{2\alpha + \sin 2\alpha}{\alpha^2 - \sin^2\alpha}} \tag{9a}$$

$$\tilde{g}(\alpha) = -1 - 3\tilde{f}(\alpha) + \tilde{f}_1(\alpha) \tag{9b}$$

$$\tilde{h}(\alpha) = 2 + 2\tilde{f}(\alpha) - \tilde{f}_1(\alpha) \tag{9c}$$

with

$$\tilde{f}_1(\alpha) = \frac{6.142 + 2.040\alpha^2 - 0.129\alpha^3}{\alpha^{3/2}} \tag{10}$$

Eq. (7) can be seen as a weight function, since it allows to determine the SIF for any stress field $\sigma_y(x)$ acting on the crack faces

$$K_I(a) = \int_0^a \sigma_y(x)\sqrt{2/(\pi a)}\, F(x/a, \alpha)\mathrm{d}x \tag{11}$$

The principle of effects superposition is then invoked (Carpinteri *et al*. 2008). The geometry we are dealing with (Fig. 4(a)) can be seen as the sum of the two cases of Figs. 4(b) and 4(c), where

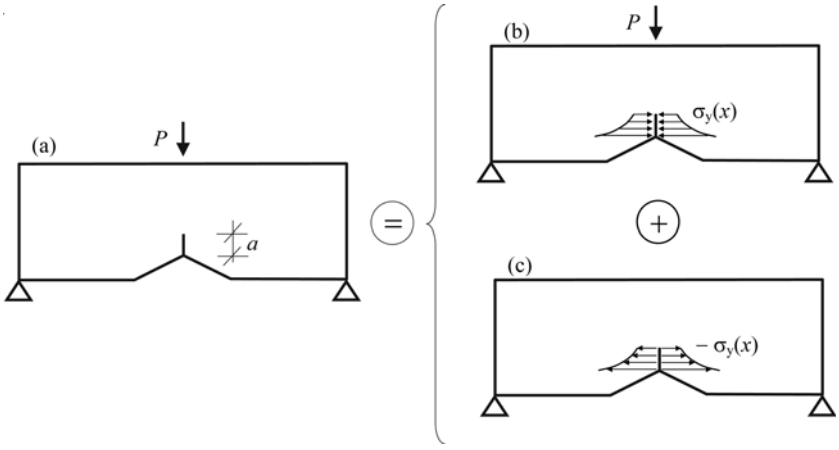

Fig. 4 Principle of effect superposition to determine the SIF of a crack at a notch tip. The SIFs of the schemes (a) and (c) are equal and the stress distribution of schemes (b) and (c) are given by Eq. (6). Observe that the geometry (b) coincides with the un-cracked case of Fig. 1

the crack faces are subjected to the stress field of the un-cracked specimen, i.e., Eq. (6). In the former scheme (Fig. 4(b)) the stresses cause crack closure and it is evident that the SIF is null. In the latter one (Fig. 4(c)) the stresses tend instead to open the crack lips; the SIF coincides with the SIF of the geometry we are interested in (Fig. 4(a)). By substituting the stress field (6) into Eq. (11)

$$K_I(a) = \psi(\omega)\frac{K_I^*}{(2\pi)^{1-\lambda}}a^{\lambda-1/2} \tag{12}$$

where

$$\psi(\omega) = \sqrt{2/\pi}[\tilde{f}(\alpha)B(\lambda,1/2)+\tilde{g}(\alpha)B(\lambda+1,1/2)+\tilde{h}(\alpha)B(\lambda+2,1/2)] \tag{13}$$

and B is the classical Beta function. The function ψ depends on the notch opening angle ω through λ and α and its values are reported in Table 6.

Concerning the dependence on the crack length, it is worthwhile to observe that Eq. (12) encompasses the limit case of an edge crack, $K_I \propto \sqrt{a}$ ($\omega = 180^o$, $\lambda = 1$) and a pre-existing crack, $K_I \propto a^0$, i.e., constant ($\omega = 0^o$, $\lambda = 0.5$). This last result is coherent with the assumption $a << d$.

Table 6 Singular exponents λ and non-dimensional functions ψ and ξ according to Eqs. (13) and (15), respectively

ω	λ	ψ	ξ
0°	0.5000	2.5066	1.0000
30°	0.5014	2.5304	0.9901
60°	0.5122	2.5399	0.9827
90°	0.5445	2.5125	0.9828
120°	0.6157	2.4231	0.9938
150°	0.7520	2.2514	1.0109
180°	1.0000	1.9870	1.0000

It is now possible to solve the system (2) by substituting Eqs. (6) and (12) into the system (2). Its solution yields the value of the finite crack extension

$$\Delta = \frac{2}{\lambda \psi^2}\left(\frac{K_{Ic}}{\sigma_u}\right)^2 \tag{14}$$

and of the generalized fracture toughness (Carpinteri *et al.* 2008)

$$K_{Ic}^{*} = \lambda^{\lambda}\left[\frac{4\pi}{\psi^2}\right]^{(1-\lambda)}\frac{K_{Ic}^{2(1-\lambda)}}{\sigma_u^{1-2\lambda}} = \xi(\omega)\frac{K_{Ic}^{2(1-\lambda)}}{\sigma_u^{1-2\lambda}} \tag{15}$$

where the function ξ has been introduced for the sake of simplicity. From Eqs. (14) and (15) it is clear that the finite crack extension Δ and the generalized toughness K_{Ic}^{*} are both function of the material parameters and of the notch opening angle ω (through ψ and λ) and, hence, structural properties. Moreover, note that K_{Ic}^{*} is intermediate between strength and toughness, being the function ξ equal to 1 for ω equal to 0^{o} and 180^{o} (Table 6).

Once K_{Ic}^{*} is known, the failure load is easily obtained; taking the ratio side by side of Eqs. (4) and (5) and using the expression (15) of the generalized fracture toughness, yields

$$\frac{P_{cr}^{\omega}}{P_{cr}^{\pi}} = \xi(\omega)\frac{f(d/b,\pi)}{f(d/b,\omega)}s^{2(1-\lambda)} \tag{16}$$

i.e., the ratio between the failure loads for a notched and an un-notched specimen is function only of the geometry and of the brittleness number s (Eq. (1)).

Note that a formula analogous to Eq. (12) providing the energy required for creating a small crack at a V-notch tip has been recently derived by Leguillon (2002). He exploited a different technique (i.e., the theory of asymptotic matching); however, he has not provided an analytic expression for the SIF of a crack at a notch tip as we have done here by means of Eqs. (12) and (13). Other fracture criteria successfully applied to notched structures have been introduced by Sih (1991), exploiting his strain energy density theory, and by Lazzarin *et al.* (2001), assuming the strain energy surrounding the notch tip as the critical parameter.

4. Comparison with experimental data

The coupled FFM criterion has been applied to the data obtained experimentally and presented in Section 2, in order to have an estimate of its effective predictive capability. Based on the values of the tensile strength, of the fracture toughness and of the values of the functions ψ and ξ provided in Table 6, the generalized fracture toughness and the finite crack extension (Eqs. (14) and (15)) are plotted vs. notch opening angle in Figs. 5 and 6, respectively.

To what concerns *test 1*, wishing to have a more complete description of the effect of the notch opening angle, a FEA was performed by using the LUSAS ® code to get the values of the shape function f (Table 4) also for geometries that were not tested i.e., for ω equal to 0^{o}, 30^{o} and 90^{o} ($d/b = 0.1$). Results are presented in Fig. 7, where the relative failure load (Eq. (16)) is plotted vs. the notch opening angle ω, together with experimental data: as it can be seen, the coupled FFM criterion yields satisfactory results. Note that it provides a minimum for notch opening angles larger than zero: this trend is in agreement with experimental data from the literature (see, for instance, Carpinteri 1987, Seweryn 1994).

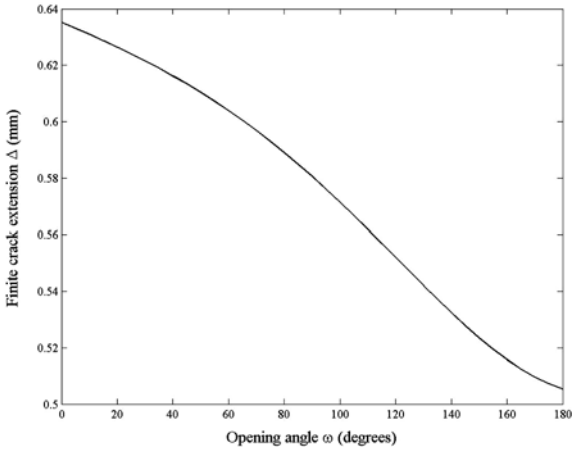

Fig. 5 Finite crack extension Δ vs. notch opening angle ω for the polystyrene specimens

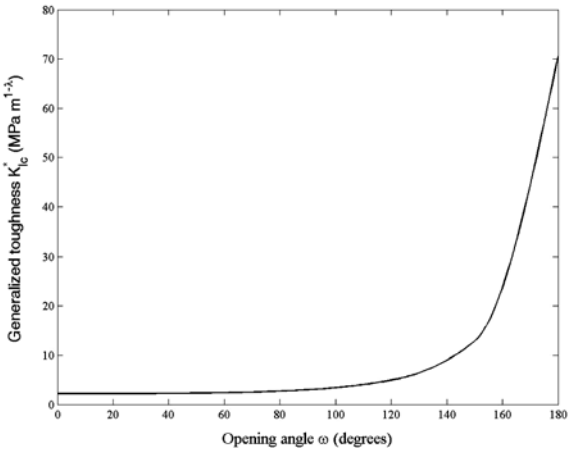

Fig. 6 Generalized toughness K^*_{Ic} vs. notch opening angle ω, according to the coupled FFM criterion for the polystyrene specimens

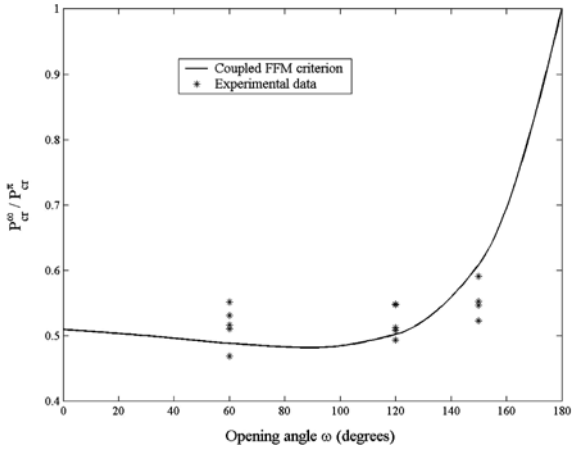

Fig. 7 Relative failure loads of the three-point bending polystyrene specimens vs. notch opening angle: experimental data and theoretical predictions (d/b = 0.1)

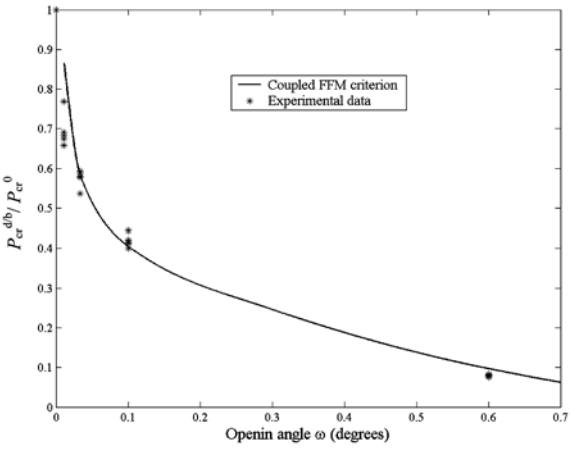

Fig. 8 Relative failure loads of the three-point bending polystyrene specimens vs. relative notch depth: experimental data and theoretical predictions (ω = 120°)

About *test 2*, Eqs. (4) and (5) can be exploited to obtain the ratio between the failure load for a given notch depth d/b, $P_{cr}^{d/b}$, and for a null one, P_{cr}^{0}, the opening angle ω being fixed

$$\frac{P_{cr}^{d/b}}{P_{cr}^{0}} = \xi(\omega)\frac{f(0,\pi)}{f(d/b,\omega)}s^{2(1-\lambda)} \tag{17}$$

Also in this case, a FEA was performed to achieve some values of the shape function f (Table 5) for geometries that were not tested: d/b = 3/10 and 9/10 (ω = 120°). Theoretical predictions based on Eq. (17) are plotted in Fig. 8, together with the experimental data of *test 2*. As it can be seen, results for intermediate geometries are in very good agreement with the experimental ones, the

maximum percentage error keeping below 3%. On the other hand, for the extreme cases d/b = 1/90 and 3/5, it rises up to 22%. Less good results for very small and very large notch depths were expected, since, in such cases, the finite crack extension tends to exceed the region of validity of the asymptotic stress field.

Eventually, test 3 shows a brittleness number s which is so high (i.e., a more ductile behaviour) that criteria based on the generalized SIF are no more applicable.

5. Conclusions

In this paper the results of a series of three-point bending tests on V-notched specimens made of polystyrene have been presented. Tests involved different notch angles, different notch depths and different sizes of the samples. Hence, a large amount of experimental data concerning different geometries is now available. The coupled FFM criterion presented in (Cornetti *et al*. 2007) is then taken into account and applied to the geometry under examination. It has been stressed that this fracture criterion derives from an energy balance and is therefore more physically sound with respect to the classical average stress criterion. In order to check its validity, predictions by the coupled FFM criterion are compared with tests results: the agreement between theory and experiments is more than satisfactory.

References

Carpinteri, A. (1981), "Static and energetic fracture parameters for rocks and concretes", *Mater. Struct.*, **14**, 151-162.

Carpinteri, A. (1987), "Stress-singularity and generalized fracture toughness at the vertex of re-entrant corners", *Eng. Fract. Mech.*, **26**, 143-155.

Carpinteri, A. and Pugno, N. (2005), "Fracture instability and limit strength conditions in structures with re-entrant corners", *Eng. Fract. Mech.*, **72**, 1254-1267.

Carpinteri, A., Cornetti, P., Barpi, F. and Valente, S. (2003), "Cohesive crack model description of ductile to brittle size-scale transition: Dimensional analysis vs. renormalization group theory", *Eng. Fract. Mech.*, **70**, 1809-1839.

Carpinteri, A., Cornetti, P., Pugno, N., Sapora, A. and Taylor, D. (2008), "A finite fracture mechanics approach to structures with sharp V-notches", *Eng. Fract. Mech.*, **75**, 1736-1752.

Cornetti, P., Pugno, N., Carpinteri, A. and Taylor, D. (2006), "Finite fracture mechanics: A coupled stress and energy failure criterion", *Eng. Fract. Mech.*, **73**, 2021-2033.

Dunn, M.L., Suwito, W. and Cunningham, S. (1997), "Fracture initiation at sharp notches: Correlation using critical stress intensities", *Int. J. Solids Struct.*, **34**, 3873-3883.

Lazzarin, P. and Zambardi, R. (2001), "A finite-volume-energy based approach to predict the static and fatigue behaviour of components with sharp v-shaped notches", *Int. J. Fract.*, **112**, 275-298.

Leguillon, D. (2002), "Strength or toughness? A criterion for crack onset at a notch", *Eur. J. Mech. A/Solids*, **21**, 61-72.

Neuber, H. (1958), *Theory of Notch Stresses*, Springer, Berlin.

Novozhilov, V. (1969), "On a necessary and sufficient condition for brittle strength", *Prik. Mat. Mek.*, **33**, 212-222.

Pugno, N. and Ruoff, N. (2004), "Quantized fracture mechanics", *Philos. Mag. A*, **84**, 2829-2845.

Seweryn, A. (1994), "Brittle fracture criterion for structures with sharp notches", *Eng. Fract. Mech.*, **47**, 673-681.

Sih, G.C. (1991), "Mechanics of fracture initiation and propagation: Surface and volume energy density applied

as failure criterion", *Engineering Applications of Fracture Mechanics*, Kluwer Academic Publisher: Dordrecht.
Sinclair, G.B., Okajima, M. and Griffin, J.H. (1984), "Path independent integrals for computing stress intensity factors at sharp notches in elastic plates", *Int. J. Numer. Meth. Eng.*, **20**, 999-1008.
Tada, H., Paris, P.C. and Irwin, G.R. (1985), *The Stress Analysis of Cracks*, Handbook, Second edition, Paris Productions Incorporated, St Louis, Missouri, USA.
Taylor, D. (1999), "Geometrical effects in fatigue: a unifying theoretical model", *Int. J. Fatig.*, **21**, 413-420.
Taylor, D. (2004), "Predicting the fracture strength of ceramic materials using the theory of critical distances", *Eng. Fract. Mech.*, **71**, 2407-2416.
Taylor, D., Cornetti, P. and Pugno, N. (2005), "The fracture mechanics of finite crack extension", *Eng. Fract. Mech.*, **72**, 1021-1038.